Modeling coarse-grained van der Waals interactions using dipole-coupled anisotropic quantum Drude oscillators

Prasanta Bandyopadhyay and Mainak Sadhukhan*

Department of Chemistry, Indian Institute of Technology Kanpur, Kanpur, India

(*mainaks@iitk.ac.in.)

(Dated: July 31, 2022)

Abstract

The Quantum Drude Oscillator (QDO) model is a promising candidate for accurately calculating the van der Waals (vdW) energies. Anisotropic QDO models have recently been used to represent molecular fragments rather than single atoms. While this model promises accurate calculation of vdW energies, there is significant room for improvements such as incorporating a proper fragmentation method, higher-order dispersion corrections, etc. The present work attempts to gauge dipole-dipole interactions' ability without fragmentation. A suitable anisotropic damping function is also introduced to work with anisotropic QDO. This revised model accurately predicts the vdW complex for the majority of the systems considered. This work indicates the limit of dipole approximation for an anisotropic QDO-based model.

I. INTRODUCTION

Capturing vdW interaction energy accurately between molecular fragments is essential for understanding phenomena governed by weak intermolecular interactions. These include interactions between biological macromolecules, soft interactions between polymer molecules among other [1–7]. Building on our previous work, we show how the interactions between anisotropic Drude oscillators can capture vdW interaction effectively and the effect of higher multipoles in such interactions.

The instantaneous quantum fluctuations of electron density, coupled with Coulomb interaction, give rise to vdW interaction between electronic fragments. In the parlance of electronic structure theory, the vdW interaction is the long-range part of dynamical correlation. Computing dynamical correlation, however, is a complex problem for even moderately large electronic systems. However, due to its omnipresence, the ability to calculate vdW interaction energy with adequate accuracy is a constant challenge to chemists. Systematic treatment of dynamical correlations, and therefore of vdW interactions, can be obtained from the post-Hartree-Fock methods such as coupled-cluster (CC), configuration interaction (CI), and random-phase approximation (RPA), perturbation theory (PT) *etc.* However, these methods have steep computational costs rendering them limited to small systems. On the other hand, density functional theory-based methods are relatively inexpensive to calculate the energies for larger systems, albeit suffering from the inadequate description of electron correlation. This happens due to the unavailability of any universally accurate exchange-correlation (XC) functionals.

To overcome this limitation, vdW corrections are added on top of the XC functionals resulting improved description of vdW interaction. Over the years, several popular methods have been devised for this purpose [8–13]. Theoretically, vdW correction can be obtained by the perturbation theory on top of the mean-field description of ground-state electron density[14]. Conventionally, the dispersion interaction can be expanded into many-body interactions as

$$E_{disp} = E^{(2)}_{disp} + E^{(3)}_{disp} + E^{(4)}_{disp} + \dots \tag{1}$$

where $E^{(n)}_{disp}$ describes the simultaneous interaction between n fragments. In all conventional theories, the fragments are individual atoms for which the electron density, as well as the polarizabilities, are isotropic. The leading term in Eq.(1) is two-body interaction $E^{(2)}_{disp}$ which dominates the

vdW interactions. Furthermore, to avoid the nonlinearity introduced by Coulomb interaction potential, it is customary to expand it into multipoles[14]. Altogether $E^{(2)}_{disp}$ is the sum of all two-body interaction terms, each derived from different multipolar interactions [15, 16]. It can be expressed as

$$E^{(2)}_{disp} = -\sum_{i<j}\left(\frac{C_{6,ij}}{R^6_{ij}} + \frac{C_{8,ij}}{R^8_{ij}} + \frac{C_{10,ij}}{R^{10}_{ij}} + \cdots\right). \tag{2}$$

Here, R_{ij} is the distance between i^{th} and j^{th} atoms. $C_{n,ij}$ are n^{th}-order dispersion coefficients between i^{th} and j^{th} atoms. These coefficients are the results of interactions between individual instantaneous multipoles. They indicate dipole-dipole ($n = 6$), dipole- quadrupole ($n = 8$), dipole-octupole and quadrupole-quadrupole interactions ($n = 10$) among others. In conjunction with Eq(2), an appropriate damping function is added to remove the singularity at short distances. All vdW corrections including Grimme's -D2 [8], -D3 [9], Tkatchenko-Scheffler(TS) [17] and many-body dispersion [12] employ empirical parameters in the damping function as well as for free atom dispersion coefficients.

A popular approach to capture vdW interactions employs quantum Drude oscillators (QDO) to model the electronic fluctuations. In these approaches, each atom is replaced by a QDO [16, 18–21]. The parameters of the resulting model Hamiltonian are set by fitting with the point polarizability from empirical sources. The interaction energies between them provide the interatomic dispersion energy. QDO model has been employed to simulate anionic water-cluster [22, 23], vibrational spectroscopy of water clusters [24], reproduce the radial probability densities for liquid noble gas atoms[25] and precursor to force-field development[26–28]. Many-Body Dispersion (MBD) method [12] is another example where one isotropic QDO per atom has been used to model electron fluctuation. This method can capture many-body effects of all orders due to the exact diagonalization of the interaction matrix [29, 30].

Recently, the anisotropic QDO model also has been successfully employed to compute the vdW interaction[13] between molecular fragments. While the results were promising, errors were introduced via (1) *ad-hoc* fragmentation scheme of the molecules, (2) the absence of higher-order multipoles, and (3) the use of isotropic damping functions. However, the relative importance of each error source was unclear in Ref.[13]. In this work, we have focused our investigation on understanding the effects of higher-order multipoles and an anisotropic damping function. To this end, we analyzed the results from our method for the A24 dataset [31] and a sub-set of complexes

taken from the NCI-Atlas dataset (D442x10)[32]. We have chosen systems where the total number of atoms is < 10. This cutoff is introduced to avoid the need for any artificial fragmentation scheme. We benchmarked our results against the interaction energy calculated *via* CCSD(T)/CBS method with large basis sets. The complexes taken from the NCI-Atlas database also provide benchmark data for potential energy curves.

This paper briefly describes the QDO model, damping function, and computational methodologies in section-II. In sectionIII we investigated the efficacy of our method on A24 and a subset of D442 datasets. We conclude the paper in section-IV with indications of a few new directions.

II. THEORY AND COMPUTATIONAL METHODS

A. Calculation of Dispersion energy by QDO

The dispersion interaction between two electronic fragments can be captured from the instantaneously induced charge-density fluctuations. These fluctuating charge densities can be modeled by three-dimensional, charge neutral, anisotropic QDOs placed at the center-of-mass of each fragment. Each QDO consists of a positive charge at the core harmonically connected with a negative charge. The total Hamiltonian ($\hat{H}_{QDO}$) between two QDOs, say A and B, is

$$\hat{H}_{QDO} = \hat{h}_A + \hat{h}_B + \hat{V}_{Coul}. \tag{3}$$

$\hat{V}_{Coul}$ is the Coulomb interaction potential between the charges of QDOs A and B. To simplify our description, we assign all charges equal to unity. The free Hamiltonian of an oscillator A ($\hat{h}_A$) with mass μ_A and frequencies $(\omega_{x,A}, \omega_{y,A}, \omega_{z,A})$ at position $\vec{r}_A = (x_A, y_A, z_A)$ is given by (in atomic units),

$$\hat{h}_A = -\frac{1}{2\mu_A}\nabla_A^2 + \frac{\mu_A}{2}(\omega_{x,A}^2 x^2 + \omega_{y,A}^2 y^2 + \omega_{z,A}^2 z^2) \tag{4}$$

with energy eigenvalues

$$E_{n,A} = (n_x + \frac{1}{2})\hbar\omega_{x,A} + (n_y + \frac{1}{2})\hbar\omega_{y,A} + (n_z + \frac{1}{2})\hbar\omega_{z,A}. \tag{5}$$

The details of the calculation of interaction energy between two anisotropic QDOs are found in the theoretical section and supporting information of Ref.[13].

The leading order interaction energy between two anisotropic QDOs can be calculated from second-order perturbation theory as,

$$E_{QDO}^{AB} = -\sum_{\mathbf{m_A}\neq 0,\mathbf{n_B}\neq 0} \frac{\langle \mathbf{0_A 0_B}|H'|\mathbf{m_A n_B}\rangle \langle \mathbf{m_A n_B}|H'|\mathbf{0_A 0_B}\rangle}{W_{\mathbf{m}0}^{A} + W_{\mathbf{n}0}^{B}} \tag{6}$$

Here, $\mathbf{m_i} = (m_x, m_y, m_z)$ is an excited state of i oscillator and $W_{\mathbf{m0}}^{i} = \hbar(m_x\omega_x + m_y\omega_y + m_z\omega_z)$. H' is the dipole part of the Coulomb interaction given by

$$H' = \sum_{\alpha}^{3}\sum_{\beta}^{3} q_A(\vec{r}_A)_\alpha T_{\alpha\beta} q_\beta(\vec{r}_B)_\beta \tag{7}$$

where,

$$T_{\alpha\beta} = \frac{3R_\alpha R_\beta - R^2\delta_{\alpha\beta}}{R^5}. \tag{8}$$

Here $R = |\vec{r}_A - \vec{r}_B|$. The polarizability tensor of anisotropic QDO A is given by,

$$\mathbf{A} = \begin{pmatrix} \frac{q_A^2}{\mu_A\omega_{x,A}^2} & 0 & 0 \\ 0 & \frac{q_A^2}{\mu_A\omega_{y,A}^2} & 0 \\ 0 & 0 & \frac{q_A^2}{\mu_A\omega_{z,A}^2} \end{pmatrix} \tag{9}$$

where q_A, μ_A, and ω_A are the charge, mass, and frequency of the QDO, respectively. Throughout this work, the values of q_A, q_B, μ_A, and μ_B are set to unity for simplicity. The frequencies along three directions *viz.* ω_x, ω_y and ω_z are obtained by fitting (Eq-(9)) with the polarizability tensor calculated at CCSD/def2-TZVPPD level.

B. Modification of damping function

The dipole-coupled dispersion energy (E_{vdW}^{ij}) between a pair of interacting QDOs (indexed as i and j) is obtained as,

$$E_{vdW}^{ij} = E_{QDO}^{ij}(R_{ij}) f_{damp}(R_{ij}) \tag{10}$$

The damping function $f_{damp}(R_{ij})$ is employed to avoid the spurious divergence at small values of R_{ij}. We have chosen a Fermi-type function

$$f_{damp}(R_{ij}) = \frac{1}{1 + exp\left[-B\left(\frac{R_{ij}}{s_r R_{ij}^{vdW}} - 1\right)\right]} \tag{11}$$

for this work. Here B and s_r are empirical parameters known as the steepness and global scaling factor, respectively. These parameters depend on the underlying XC functionals[33]. In some works, another empirical parameter s_6 has also been introduced [8, 9, 33] in the $f_{damp}(R_{ij})$. To reduce the number of empirical parameters, we have not used it in the present work. Additionally, the introduction of s_6 provides a constant and spurious modulation of vdW energy in the very long-range[33]. For i^{th} and j^{th} molecular fragment pair, we computed R_{ij} as the distance between their centers of mass. R_{ij}^{vdW} is the sum of vdW radii of the i^{th} fragment (R_i^{vdW}) and j^{th} fragment (R_j^{vdW}). In our earlier work[13], the isotropic vdW radius of an anisotropic fragment is calculated from the power-law relation between point polarizability and vdW radii. [34]. The expression is given below (in atomic units),

$$R^{vdW} = 2.54\alpha^{1/7} \tag{12}$$

where, $\alpha = (1/3)\,\mathrm{Tr}\{\mathbf{A}\}$.

Since, in general, a molecular fragment is not spherically symmetric, the concept of anisotropic vdW radii has been introduced in the present work. Individual vdW radii along each direction are computed by

$$\begin{aligned} R_{(x)}^{vdW} &= 2.54\alpha_{xx}^{1/7} \\ R_{(y)}^{vdW} &= 2.54\alpha_{yy}^{1/7} \\ R_{(z)}^{vdW} &= 2.54\alpha_{zz}^{1/7}. \end{aligned} \tag{13}$$

The α_{xx}, α_{yy} and α_{zz} terms are the diagonal elements of the dipole polarizability tensor of the molecule/fragment. Note that for isotropic case, $\alpha_{xx} = \alpha_{yy} = \alpha_{zz}$ producing isotropic vdW radius R^{vdW} given by Eq.(12).

This anisotropic vdW radii of the fragment allow the interaction energy to differ in different directions. We also optimized the B and s_r parameters for this work. The detailed analysis is provided in section III.

To obtain the components of the total interaction energy, SAPT2+(3)δmp2 [35] (suggested in benchmark study in Ref. [36]) calculations are carried out with aug-cc-pVTZ (aug-cc-pVTZ-PP for atoms heavier than Kr)[37, 38] basis set. The segregation of interaction energy is performed

by the following equation, [35]

$$E_{IE}^{SAPT2+(3)\delta MP2} = E_{IE}^{SAPT2} + \left[E_{disp}^{(21)} + E_{disp}^{(22)}\right]_{disp} + \left[E_{elst,r}^{(13)}\right]_{elst} + \left[E_{disp,r}^{(30)}\right]_{disp} + E_{MP2} - E_{IE}^{SAPT2} \tag{14}$$

The interaction energies at PBE/def2-QZVPPD [39, 40] with dispersion correction -D2[8] and -D3[9] are calculated with Turbomole 7.5 [41],static polarizability (at CCSD/def2-TZVPPD [40] level) and SAPT2+(3)δmp2 calculations are performed with Psi4 [42]. It must be mentioned here that static polarizability tensors were calculated previously at a higher zeta basis, def2-QZVPPD[13]. However, we have compared the output for both TZ and QZ showing quantitatively similar results. The calculations of the electron density differences, provided in sectionIII C 1, are performed with Multiwfn [43] and plotted with VMD [44] at 0.0002 a.u. iso-density value.

III. RESULTS AND DISCUSSION

A. Estimation of anisotropy in A24 dataset

In order to verify the anisotropic nature of the electron density of the monomers of A24 dataset, we have calculated the vdW radii in all three directions ($R_{(x)}^{vdW}$, $R_{(y)}^{vdW}$ and $R_{(z)}^{vdW}$) using Eq(13). The different vdW radii for the monomers of the A24 dataset in three different directions are provided in Table-III A. 'Ar' atom is found to be perfectly isotropic, while water, ammonia, HCN, HF, methane, and borane are nearly isotropic. Moderate anisotropy is observed for the rest of the monomers. We have also provided the vdW radii for a few monomers of the D442X10 dataset in the lower panel of Table-III A. Note that the change in anisotropy is directly correlated with the chain length for long-chain molecules, thereby highlighting the necessity of an anisotropic damping function.

Monomers	R_x^{vdW}	R_y^{vdW}	R_z^{vdW}
Water	3.51	3.52	3.49
Ammonia	3.68	3.73	3.68
HCN	3.69	3.69	3.95
HF	3.21	3.21	3.31
Methane	3.79	3.79	3.79
HCHO	3.95	3.67	3.82
Ethene	4.01	3.95	4.21
Ethyne	3.85	4.14	3.85
Borane	3.85	3.71	3.85
Ethane	4.14	4.07	4.07
Ar	3.58	3.58	3.58
diphosphene	4.69	4.36	4.42
CS_2	3.97	4.15	4.05
P_4	4.85	4.85	4.85
CO_2	4.01	3.75	3.65
diphosphine	4.63	4.44	4.53
butadyine	4.62	4.17	4.30
propyne	4.19	4.32	4.13
diazene	3.96	3.86	3.67
methylazide	4.53	4.10	4.12

TABLE I. Anisotropy of vdW radii of the monomers. All values are in atomic units and approximated to second decimal places.

We optimized B and s_r parameters by minimizing the difference between reference CCSD(T)/CBS and PBE-QDO such that,

$$\varepsilon = E_{CCSD(T)/CBS} - (E_{PBE} + E_{vdW}^{QDO}) \tag{15}$$

is minimized. Here, E_{PBE} and E_{vdW}^{QDO} are interaction energies from PBE functional and QDO model, respectively. In reality, however, ε should always be negative for the present method due

to the absence of higher-order multipoles in our description. We have minimized ε for complexes in the A24 database to get the optimal B and s_r using the differential evolution method in scipy[45]. The optimized value of B and s_r for PBE functional are found to be 16 and 0.8, respectively. The inclusion of higher-order multipole is expected to alter these values and will be the subject of further studies.

B. Application to A24 dataset

Utilizing these optimized values, the PBE-QDO energy for the A24 dataset are calculated. The deviation of interaction energy from the reference CCSD(T)/CBS values for PBE, PBE-D2, PBE-D3 and PBE-QDO methods are presented in the Fig-1.

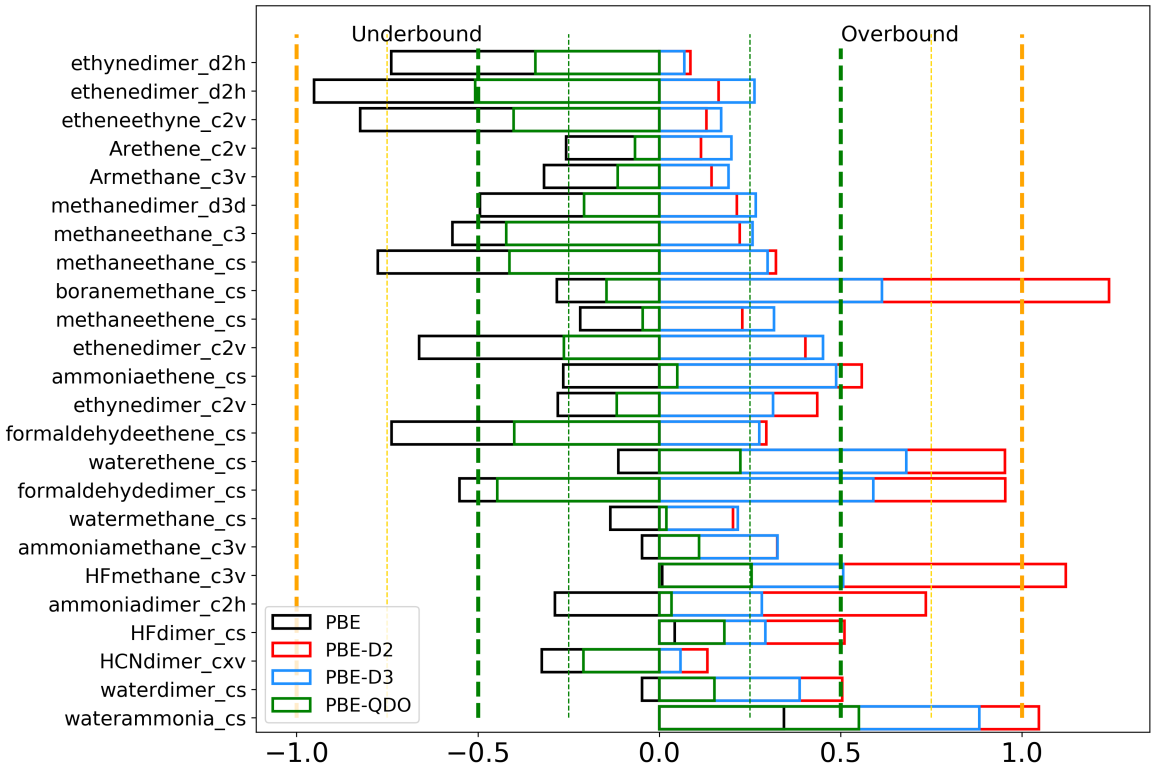

FIG. 1. Deviation (in kcal/mol) from CCSD(T)/CBS of PBE, PBE-D2, PBE-D3 and PBE-QDO.

Except for the water···ammonia (Cs), HF dimer (Cs), and HF···methane (C3v) complexes, interaction energy calculated with PBE functional provides under-binding (more positive than the actual CCSD(T) interaction energies). We computed basis set superposition error (BSSE) for all complexes by counterpoise method (CP)[46]. We found negligible corrections arising due to

BSSE for all systems (largest BSSE is found for ethene dimer (D2h) as ≈ 0.0000533 Hartree or ≈ 0.0334 kcal/mol) [47]. In all systems, the PBE-D3 method (blue vertical bars in Fig.1) shows better agreement with reference interaction energy than the -D2 method. However, these two methods generally overestimate the interaction energy. On the contrary, the PBE-QDO method (green vertical bars in Fig.1) shows better agreement with the benchmark results. The only exception to this trend is ethene dimer (D2h), where the deviation from the reference value is slightly larger than 0.5 kcal/mol. In most complexes, PBE-QDO underestimates the interaction energy emphasizing the role of higher multipole moments. The statistical analysis of errors due to PBE, PBE-D2, PBE-D3, and PBE-QDO are given in Table-III B. Overall, for the A24 dataset, -the D2 correction on PBE deteriorates the result, while -the D3 correction recovers the accuracy. We have also compared the root mean squared deviation value for PBE and PBE-D2 results with results from our method (cf. Ref.[48]), which are also provided in Table-III B in parentheses.

TABLE II. Statistical analysis of error by PBE, PBE-D2, PBE-D3 and PBE-QDO with respect to benchmark CCSD(T)/CBS data of A24 dataset.

-	PBE	PBE-D2	PBE-D3	PBE-QDO
MAE[a]	0.386	0.460	0.350	0.236
MRE[b]	0.405	0.308	0.286	0.204
MARE[c]	0.007	0.009	0.006	0.004
RMSD[d]	0.473(0.46)[e]	0.578(0.59)[e]	0.399	0.284

[a] Mean Absolute Error (in kcal/mol); [b] Mean Relative Error; [c] Mean Relative Absolute Error; [d] Root Mean Squared Deviation (in kcal/mol); [e] Data obtained from Ref.[48]

C. Calculation of D442x10 dataset

To further our investigation, we have chosen 120 small (number of atoms < 10) molecular systems from D442X10 dataset[32]. These include systems of diverse electronic natures such as noble gas atoms, P_4(number of atoms = 4), CH_nX_n (n = 1,2,3; X=halogens and number of atoms = 5), S_6 (number of atoms = 6) *etc*. The interaction energy curve (IEC) $H_2\cdots P_4$ and $P_4\cdots P_4$ complexes are shown in Fig-2. The 10-point IECs show the interaction energies at distances $R_{scaled} = \gamma R_{eq}$ where γ is the scale factor and R_{eq} is the equilibrium distance. The IEC of $H_2\cdots P_4$ shows that

PBE-QDO (blue curve) accurately describes the interaction energies calculated at CCSD(T) (red curve) at all distances of the IEC. PBE does not show almost any binding, while both PBE-D2 and PBE-D3 significantly overbind. Furthermore, PBE-D2 and PBE-D3 methods can not predict the correct position of the IEC minimum. For $P_4 \cdots P_4$ PBE functional can not predict any binding as well. While PBE-QDO recovers some binding energy compared to PBE, the binding is still vastly underestimated. PBE-D2 and PBE-D3 fare better than PBE-QDO here but still fail to reproduce the accurate binding energy curve. Interestingly, PBE-D2 performs better than PBE-D3, which is counter-intuitive. Since our method does not include any higher order multipole, their explicit inclusion in the future is expected to correct our results. Further analysis in sectionIII C 1 indicates that quadrupole-quadrupole interaction may play a significant role in capturing correct binding energy for this system. IEC for all other complexes is given in Supporting Information (SI).

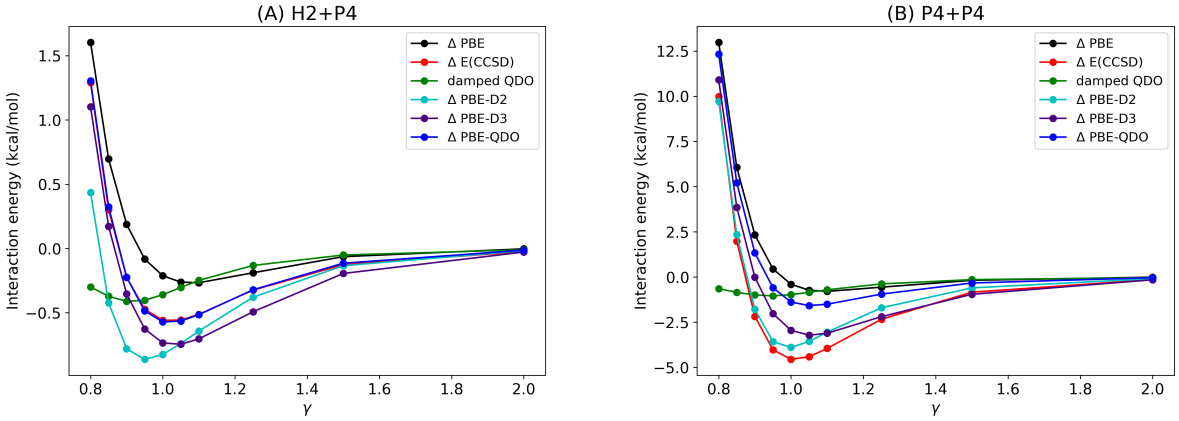

FIG. 2. IEC (in kcal/mol) for $H_2 \cdots P_4$ (A:) and $P_4 \cdots P_4$ (B:) complexes against scaled distance.

In almost all systems considered in this dataset, -D2 and -D3 corrections over-bind the complexes, while QDO correction under-binds them, following the same trend observed for the A24 dataset. This problem is quite amenable for our case since the two-body interactions due to higher multipole are all negative and expected to reduce the error. However, similar corrections to PBE-D2 or PBE-D3 will increase the error. Only the inclusion of three-body interactions may reduce the error in these later methods. For a few systems, PBE-QDO correction also produces over-binding. However, the amounts of such overbinding are generally negligible except for diazene$\cdots F_2$ complex (see Supporting information). However, this particular complex is already over-bound by PBE itself (BSSE correction ≈ 0.012 kcal/mol and therefore cannot compensate for the error), and therefore, any vdW correction based on two-body interaction is bound to worsen the situa-

tion. Among 120 complexes considered, PBE-QDO underestimates 18 complexes by more than 1 kcal/mol. For these cases, PBE also underbinds significantly. As a result, our method could not stand up to the challenge of correcting all errors introduced by the underlying XC-functional.

For the 120 complexes taken from D442, we have analyzed our results in terms of MAE, MRE, MARE, and RMSD (Table-III C). The results from bare PBE functional are the least accurate. While the rectification by the PBE-QDO method is still less than PBE-D2 and PBE-D3, the consistent over-binding by both PBE-D2 and PBE-D3 methods indicates an over-correction by the corresponding damping functions. However, if we exclude the 18 outliers from the analysis (values in parentheses in Table III C), PBE and PBE-QDO show significantly improved results. Moreover, the corrections due to PBE-QDO becomes at par with the PBE-D2 and PBE-D3. We will separately analyze some of these cases in sectionIII C 1. As seen from the detailed plots in SI, PBE-QDO consistently underbinds the complexes emphasizing the role of higher multipoles.

The problem of using isotropic vdW radii for fragments in our damping function has already been discussed before in III. To clarify further, a comparison between the results obtained by an isotropic (PBE-QDO$_{iso}$) and an anisotropic (PBE-QDO$_{aniso}$) damping function are presented in Table-III C. No significant improvement is observed between PBE and PBE-QDO$_{iso}$ has been observed, rendering the use of the isotropic damping function useless for our purpose. Therefore, the anisotropic damping function is an essential element of our model. However, note that the source of anisotropy is the vdW radii rather than any arbitrary empirical parameters. As a result, we are not increasing the number of empirical parameters in our present work.

1. Analysis of electron density difference

To investigate the reasons for large deviations in interaction energies for 18 outlier complexes, electron density differences (EDD) have been computed for them. EDD is computed as the difference in density of dimer and that of monomers as $\Delta\rho = \rho_{AB}(\mathbf{r}) - (\rho_A(\mathbf{r}) + \rho_B(\mathbf{r}))$ where ρ_{AB}, ρ_A and ρ_B are electron densities of the dimer AB, monomer A and monomer B, respectively. The EDD for four complexes is presented in Fig3. Our method accurately describes interaction energy for $P_4 \cdots H_2$ complex (≈ 0.01 kcal/mol over-binding). The density deformation at equilibrium distance is minimal for this complex as well. As a result, the frequency parametrization of QDO is expected to be unaltered at different inter-monomer distances, thereby explaining our method's

TABLE III. Statistical analysis of error by PBE, PBE-D2, PBE-D3 and PBE-QDO with respect to benchmark CCSD(T)/CBS data of D442 dataset.[e]

-	PBE	PBE-D2	PBE-D3	PBE-QDO$_{aniso}$[f]	PBE-QDO$_{iso}$[g]
MAE[a]	0.674(0.400)	0.238(0.217)	0.210(0.181)	0.465(0.244)	0.637(0.366)
MRE[b]	0.659(0.616)	0.685(0.781)	0.679(0.775)	0.589(0.571)	0.675(0.639)
MARE[c]	0.007(0.007)	0.002(0.004)	0.002(0.003)	0.005(0.004)	0.007(0.006)
RMSD[d]	1.056(0.564)	0.313(0.288)	0.298(0.236)	0.778(0.341)	1.018(0.523)

[a] Mean Absolute Error (in kcal/mol); [b] Mean Relative Error; [c] Mean Relative Absolute Error; [d] Root Mean Squared Deviation (in kcal/mol); [e] Values in parentheses are calculated for the same dataset after removing 18 outliers appeared for PBE-QDO. [f] Values obtained with anisotropic damping function [g] Values obtained with isotropic damping function; the form of which is shown in Ref.[13].

success. For $P_4\cdots P_4$, $F_2\cdots$diazene and $S_6\cdots Br_2$ the change in density is significant. Therefore, the parametrization of QDO model is expected to change for these systems with the change in inter-monomer distance. Since our parameterizations are done for free monomer systems, a significant deviation from the accurate interaction energy at equilibrium is expected. Indeed, except for the $P_4\cdots H_2$ complex, all other complexes show such behavior. Interestingly, while the electron density has changed by a significant amount for $F_2\cdots$diazene at equilibrium, our method does not fare very bad here (≈ 0.7 kcal/mol over-binding). We will investigate the reason for this behavior in the next section. Additionally, the EDD analysis reveals quadrupolar charge distribution compared to the monomer electron density for the later three complexes. Since our method is only limited to dipole-coupling, it could not capture the quadrupole-quadrupole interaction leading to the above-mentioned failure.

2. *SAPT analysis*

The success of our method for the $F_2\cdots$diazene complex, despite the large charge redistribution at equilibrium distance compared to the individual monomers, dictated us to investigate the relative importance of dispersion interaction in these complexes. We compute the relative dispersion contribution R_{disp} as

$$R_{disp} = \frac{E_{dispersion}}{E_{electrostatic} + E_{induction} + E_{dispersion}} \times 100. \tag{16}$$

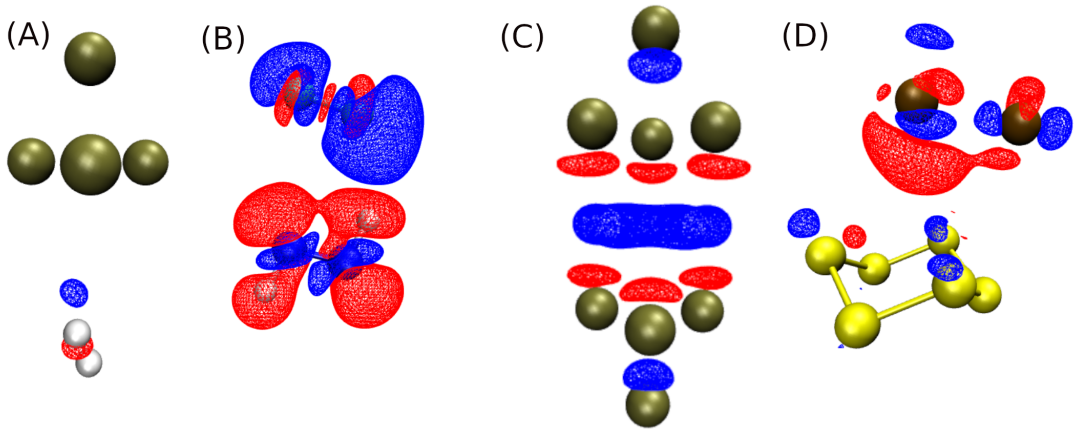

FIG. 3. EDD plot for (A) $P_4\cdots H_2$, (B) $F_2\cdots$diazene, C: $P_4\cdots P_4$ and D: $S_6\cdots Br_2$ at 0.0002 a.u. isodensity value. Blue and red mesh denotes increase and decrease of density respectively.

where $E_{dispersion}$, $E_{electrostatic}$ and $E_{induction}$ are dispersion, electrostatic and induction contributions to the total interaction energy. We obtained these contributions *via* $SAPT2+(3)\delta MP2$ analysis. We also computed R_{disp} for three well behaved systems (Ne$\cdots$Ne, $P_4\cdots H_2$ and $P_4\cdots N_2$) for comparison. Table III C 2 summarizes these results.

All 18 systems show higher dispersion contribution towards total interaction energy compared to $F_2\cdots$diazene. Therefore, the overall effect of the absence of quadrupole moment in our description does not affect the accuracy for the case of $F_2\cdots$diazene. R_{disp} for last three complexes in Table III C 2 are also large. However, since the electron density does not deform significantly for these complexes at equilibrium distance compared to their monomeric counterpart, we obtain good results for these systems. This analysis indicates that for systems with (1) large R_{disp} and (2) large density deformation, our model requires contributions from quadrupole moments to attain accuracy. Other systems, which constitute the majority of the concerned databases, are well described by our method.

3. *Performance of PBE-QDO method for varying system sizes*

It is imperative to understand the effect of system size on the underlying density functional and the QDO correction over it. To do so, We have analyzed the deviations of PBE and PBE-QDO interaction energies from the CCSD(T)/CBS (at equilibrium distance) as a function of the

TABLE IV. Symmetry Adapted Perturbation Theory 2+(3)$\delta MP2$ analysis for selected complexes. All values (except %Dispersion) are in kcal/mol.

Complexes	Electrostatic	Exchange	Induction	Dispersion	Total	R_{disp}
$CS_2\cdots Br_2$	-1.1783	3.2325	-0.1099	-4.0794	-2.1351	75.99
$S_6\cdots Br_2$	-3.1654	7.6502	-0.2342	-7.1029	-2.8523	67.63
$P_4\cdots Br_2$	-2.0290	5.2141	-0.1524	-5.6813	-2.6487	72.26
diphosphene $\cdots CCl_4$	-2.4673	6.3295	-0.4387	-5.3467	-1.9233	64.79
$P_4\cdots CHF_3$	-0.9472	2.5601	0.0722	-3.1853	-1.5001	75.75
$CO_2\cdots I_2$	-1.0192	2.6313	-0.2259	-2.9071	-1.5209	70.01
$CO_2\cdots CH_2Br_2$	-2.5555	3.8438	-0.4194	-3.8358	-2.9670	56.32
$CO_2\cdots CHCl_3$	-1.3044	2.8603	-0.1794	-3.3182	-1.9418	69.10
hydrogenazide$\cdots CI_4$	-3.1590	6.8818	-1.885	-5.7501	-3.9123	53.27
hydrogenazide$\cdots CHCl_3$	-2.3649	4.3498	-1.1986	-3.8505	-3.0642	51.93
$P_4\cdots P_4$	-4.5426	11.7006	-0.8545	-12.5611	-6.2578	69.94
$CO_2\cdots CS_2$	-1.0933	2.3488	-0.2143	-2.7252	-1.6840	67.57
$CO_2\cdots$diphosphine	-2.1045	3.6130	-0.3752	-3.2971	-2.1638	57.07
$CH_2I_2\cdots I_2$	-2.2648	6.2515	-0.7205	-6.3128	-3.0466	67.89
$CHBr_3\cdots Br_2$	-4.1919	5.4122	1.7359	-5.2362	-2.2799	68.07
$CS_2\cdots I_2$	-1.577	4.1749	-0.1632	-4.9966	-2.5619	74.17
Xe$\cdots CH_2I_2$	-0.9690	2.8932	-0.3467	-3.162	-1.5844	70.61
Kr$\cdots CHI_3$	-1.1606	3.0346	-0.1174	-2.9697	-1.2131	69.91
$F_2\cdots$diazene	-0.3636	1.2515	-0.1589	-1.1662	-0.4373	45.55
$P_4\cdots H_2$	-0.3342	1.3988	-0.1225	-1.4453	-0.5032	76.99
$P_4\cdots N_2$	-0.6981	2.4179	0.0459	-2.6746	-0.9089	80.39
Ne$\cdots$Ne	-0.0262	0.1116	0.0007	-0.1301	-0.0439	83.61

system size. Here we employed two metrics of system size. In the first case, we defined the size

(reminiscent of steric size) of the complexes as their average vdW radii $R_{complex}$ defined as

$$\begin{aligned} \bar{R}_A &= (R^{vdW}_{A,x} + R^{vdW}_{A,y} + R^{vdW}_{A,z})/3 \\ \bar{R}_B &= (R^{vdW}_{B_{(x)}} + R^{vdW}_{B_{(y)}} + R^{vdW}_{B_{(z)}})/3 \\ R_{complex} &= \bar{R}_A + \bar{R}_B \end{aligned} \tag{17}$$

for monomers A and B. Here $R^{vdW}_{\alpha,i}$ is the vdW radius of α monomer along i direction (cf. Eq.(13)). The result is shown in Fig.4(A). We have also analysed the deviation in interaction energy from bare PBE functional (cf. Eq.(15)) as

$$\varepsilon_0 = E_{CCSD(T)/CBS} - E_{PBE} \tag{18}$$

in the same plot. The other metric of system size used here is the total number of the electrons N_{dimer} shown in Fig.4(B). The variation of ε and ε_0 with $R_{complex}$ show a polynomial growth of error for PBE as well as for PBE-QDO. A polynomial fit of the form

$$\Delta E = a \times R^b_{complex} + c \tag{19}$$

were used to quantify the nature of growth. Here, ΔE is the shorthand for ε and ε_0. The fitting parameters a,b and c are provided in Table-V:

Method	a	b	c
PBE	-1.5×10^{-08}	8.58	0.23
PBE-QDO	-2.0×10^{-09}	9.36	0.21

TABLE V. Fitting parameters for scatter plot of 4(a)

We can see from Fig.4(A) that for both PBE-QDO and PBE , the exponent of growth is quite large. However, PBE-QDO works better due to small a value. Visual inspection of the plot clearly shows that the the correction by QDO model is comparatively larger for larger complex size while still being inadequate to recover the error incurred by the PBE functional. Therefore, a better XC functional with smaller exponent b is required to be working with present version of our method. We can see that above around 8.25 bohr, the PBE-QDO method start failing to capture the chemical accuracy. Similar threshold of 50 electrons can also be obtained from Fig.4(B).

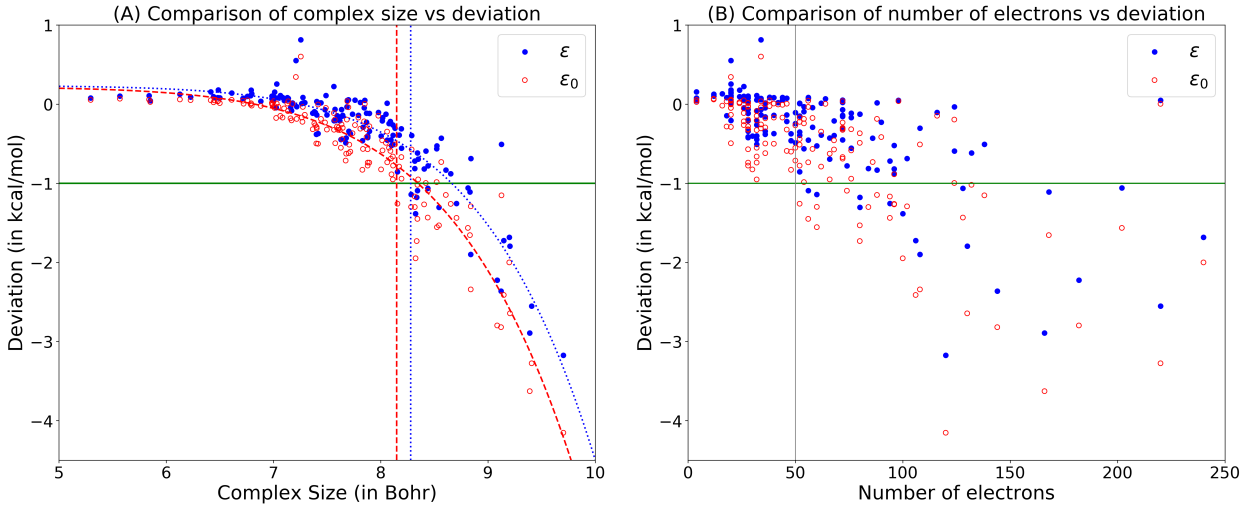

FIG. 4. A: Size vs accuracy comparison, B: number of electrons vs accuracy between PBE and PBEQDO for reduced D442 dataset. ε and ε_0 are defined in Eq.(15) and Eq.(18) respectively.

IV. CONCLUSION

In summary, we have utilized the anisotropic QDO model coupled with an anisotropic damping function to capture the intermolecular vdW interactions. The method is applied to A24 and a reduced version of the D442X10 dataset without fragmenting the monomers, thus eliminating errors originating from fragmentation. The only fitting parameter used in the anisotropic damping function depends upon the XC functional. We have analyzed this model's accuracy and limitations at the dipole-dipole interaction limit. Our method fairs well for the large majority of 144 complexes considered here. We have also analyzed the reasons for our model's failures for these 18 complexes via SAPT and electron density difference analyses. We found that the electron density deforms at the equilibrium distance for all such cases compared to the monomers. Particularly, it affects the cases where the dispersion contribution to total interaction energy is significant. These results suggest that the higher-multipole corrections and an on-the-fly QDO parametrization procedure are required to improve our method further. We will consider these challenges in future works. With this work, we have pushed our dipole-coupled model to its limit and opened the directions for further work.

CONFLICTS OF INTEREST

There are no conflicts to declare.

DEDICATION

This work is dedicated to Prof. B. M. Deb, one of the earliest doyens of theoretical chemistry research in India.

ACKNOWLEDGMENTS

We wish to acknowledge the support of Prof. Jan Rezac from Institute of Organic Chemistry and Biochemistry, Czech Academy of Sciences for fruitful discussions regarding D442x10 dataset. PB thanks IIT Kanpur for an Institute Post-Doctoral Fellowship. MS thanks SERB grant No. SRG/2019/000369 for computational support and Debashree Manna for numerous helpful discussions.

---

[1] J. F. Dobson and T. Gould, Journal of Physics: Condensed Matter **24**, 073201 (2012).

[2] M. Stöhr, T. Van Voorhis, and A. Tkatchenko, Chemical Society Reviews **48**, 4118 (2019).

[3] J. Hermann, R. A. DiStasio, and A. Tkatchenko, Chemical Reviews **117**, 4714 (2017).

[4] K. Autumn, M. Sitti, Y. A. Liang, A. M. Peattie, W. R. Hansen, S. Sponberg, T. W. Kenny, R. Fearing, J. N. Israelachvili, and R. J. Full, Proceedings of the National Academy of Sciences **99**, 12252 (2002).

[5] B. Rozitis, E. MacLennan, and J. P. Emery, Nature **512**, 174 (2014).

[6] J. Hoja, A. M. Reilly, and A. Tkatchenko, WIREs Computational Molecular Science **7**, e1294 (2017), https://wires.onlinelibrary.wiley.com/doi/pdf/10.1002/wcms.1294.

[7] D. Chandler, Nature **437**, 640 (2005).

[8] S. Grimme, Journal of Computational Chemistry **27**, 1787 (2006).

[9] S. Grimme, J. Antony, S. Ehrlich, and H. Krieg, The Journal of Chemical Physics **132**, 154104 (2010).

[10] S. Grimme, J. Antony, T. Schwabe, and C. Mück-Lichtenfeld, Org. Biomol. Chem. **5**, 741 (2007).

[11] A. Tkatchenko, R. A. DiStasio, R. Car, and M. Scheffler, Physical Review Letters **108**, 236402 (2012).

[12] A. Tkatchenko, A. Ambrosetti, and R. A. DiStasio, The Journal of Chemical Physics **138**, 074106 (2013).

[13] P. Bandyopadhyay, Priya, and M. Sadhukhan, Phys. Chem. Chem. Phys. **24**, 8508 (2022).

[14] A. J. Stone, *The Theory of Intermolecular Forces*, 2nd ed. (Oxford University Press).

[15] A. Otero-de-la Roza, L. M. LeBlanc, and E. R. Johnson, Physical Chemistry Chemical Physics **22**, 8266 (2020).

[16] A. Jones, J. Crain, F. Cipcigan, V. Sokhan, M. Modani, and G. Martyna, Molecular Physics **111**, 3465 (2013).

[17] A. Tkatchenko and M. Scheffler, Physical Review Letters **102**, 073005 (2009).

[18] V. K. Voora, J. Ding, T. Sommerfeld, and K. D. Jordan, Journal of Physical Chemistry B **117**, 4365 (2013).

[19] M. Sadhukhan and F. R. Manby, Physical Review B **94**, 115106 (2016).

[20] T. Odbadrakh, V. Voora, and K. Jordan, Chemical Physics Letters **630**, 76 (2015).

[21] K. D. Jordan and F. Wang, Annual Review of Physical Chemistry **54**, 367 (2003).

[22] T. Sommerfeld and K. D. Jordan, The Journal of Physical Chemistry A **109**, 11531 (2005).

[23] T. Sommerfeld, A. DeFusco, and K. D. Jordan, The Journal of Physical Chemistry A **112**, 11021 (2008).

[24] T. O. Tuguldur, "Applications of the quantum drude oscillator model for dispersion interactions and vibrational spectroscopy of charged water clusters," (2018).

[25] A. Jones, F. Cipcigan, V. P. Sokhan, J. Crain, and G. J. Martyna, Physical Review Letters **110**, 227801 (2013).

[26] T. Chen and T. A. Manz, RSC Advances **9**, 36492 (2019).

[27] J. Huang, P. E. M. Lopes, B. Roux, and A. D. MacKerell, The Journal of Physical Chemistry Letters **5**, 3144 (2014).

[28] A. Savelyev and A. D. MacKerell, Journal of Computational Chemistry **35**, 1219 (2014).

[29] M. Stöhr and A. Tkatchenko, Science Advances **5**, eaax0024 (2019).

[30] J. Claudot, W. J. Kim, A. Dixit, H. Kim, T. Gould, D. Rocca, and S. Lebègue, The Journal of Chemical Physics **148**, 064112 (2018).

[31] J. Řezáč and P. Hobza, Journal of Chemical Theory and Computation **9**, 2151 (2013), pMID: 26583708.

[32] J. Řezáč, Phys. Chem. Chem. Phys. **24**, 14780 (2022).

[33] P. Jurecka, J. Cerný, P. Hobza, and D. R. Salahub, Journal of Computational Chemistry **28**, 555 (2007).

[34] D. V. Fedorov, M. Sadhukhan, M. Stöhr, and A. Tkatchenko, Physical Review Letters **121**, 183401 (2018), arXiv:1803.11507.

[35] T. M. Parker, L. A. Burns, R. M. Parrish, A. G. Ryno, and C. D. Sherrill, The Journal of Chemical Physics **140**, 094106 (2014), https://doi.org/10.1063/1.4867135.

[36] E. G. Hohenstein and C. D. Sherrill, The Journal of Chemical Physics **133**, 014101 (2010), https://doi.org/10.1063/1.3451077.

[37] B. P. Pritchard, D. Altarawy, B. Didier, T. D. Gibson, and T. L. Windus, Journal of Chemical Information and Modeling **59**, 4814 (2019), pMID: 31600445, https://doi.org/10.1021/acs.jcim.9b00725.

[38] A. K. Wilson, T. van Mourik, and T. H. Dunning, Journal of Molecular Structure: THEOCHEM **388**, 339 (1996).

[39] J. P. Perdew, M. Ernzerhof, and K. Burke, The Journal of Chemical Physics **105**, 9982 (1996).

[40] F. Weigend and R. Ahlrichs, Physical Chemistry Chemical Physics **7**, 3297 (2005).

[41] S. G. Balasubramani, G. P. Chen, S. Coriani, M. Diedenhofen, M. S. Frank, Y. J. Franzke, F. Furche, R. Grotjahn, M. E. Harding, C. Hättig, A. Hellweg, B. Helmich-Paris, C. Holzer, U. Huniar, M. Kaupp, A. Marefat Khah, S. Karbalaei Khani, T. Müller, F. Mack, B. D. Nguyen, S. M. Parker, E. Perlt, D. Rappoport, K. Reiter, S. Roy, M. Rückert, G. Schmitz, M. Sierka, E. Tapavicza, D. P. Tew, C. van Wüllen, V. K. Voora, F. Weigend, A. Wodyński, and J. M. Yu, The Journal of Chemical Physics **152**, 184107 (2020).

[42] D. G. A. Smith, L. A. Burns, A. C. Simmonett, R. M. Parrish, M. C. Schieber, R. Galvelis, P. Kraus, H. Kruse, R. Di Remigio, A. Alenaizan, A. M. James, S. Lehtola, J. P. Misiewicz, M. Scheurer, R. A. Shaw, J. B. Schriber, Y. Xie, Z. L. Glick, D. A. Sirianni, J. S. O'Brien, J. M. Waldrop, A. Kumar, E. G. Hohenstein, B. P. Pritchard, B. R. Brooks, H. F. Schaefer, A. Y. Sokolov, K. Patkowski, A. E. DePrince, U. Bozkaya, R. A. King, F. A. Evangelista, J. M. Turney, T. D. Crawford, and C. D. Sherrill, The Journal of Chemical Physics **152**, 184108 (2020).

[43] T. Lu and F. Chen, Journal of Computational Chemistry **33**, 580 (2012), https://onlinelibrary.wiley.com/doi/pdf/10.1002/jcc.22885.

[44] W. Humphrey, A. Dalke, and K. Schulten, Journal of Molecular Graphics **14**, 33 (1996).

[45] R. Storn and K. Price, Journal of Global Optimization **11**, 341 (1997).

[46] S. Boys and F. Bernardi, Molecular Physics **19**, 553 (1970), https://doi.org/10.1080/00268977000101561.

[47] In water$\cdots$ammonia (Cs) complex, the BSSE energy is ≈ -0.00388 kcal/mol indicating that the overestimation of interaction energy in water$\cdots$ammonia (Cs) complex is not due to the BSSE.

[48] N. Mardirossian and M. Head-Gordon, Phys. Chem. Chem. Phys. **16**, 9904 (2014).